

光学学报

基于过焦扫描光学显微术的套刻误差检测方法研究

刘浩¹, 王劲松^{1*}, 石俊凯^{2**}, 李冠楠², 陈晓梅², 周维虎²¹长春理工大学光电工程学院, 吉林 长春 130022;²中国科学院微电子研究所光电技术研发中心, 北京 100029

摘要 针对套刻误差测量,提出了一种基于过焦扫描光学显微技术(TSOM)结合深度学习模型的测量方法,利用传统光学显微镜采集不同偏移量的套刻标识图像,建立TSOM图集,通过卷积神经网络模型对套刻标识偏移量进行回归预测,最终得到套刻误差预测结果的误差小于0.1 nm,重复精度(3σ)优于0.25 nm。实验结果表明,基于TSOM结合深度学习的测量方法实现了亚纳米级精度套刻误差测量。该方法可以为优化光刻工艺提供有力的支撑。

关键词 测量; 套刻误差; 过焦扫描光学显微技术; 深度学习; 无损检测

中图分类号 TH744

文献标志码 A

DOI: 10.3788/AOS231900

1 引言

集成电路(IC)产业的快速发展是国家现代信息化建设、国民经济和社会持续健康发展的重要支撑^[1]。在过去十年中,IC技术伴随着复杂3D器件结构的使用取得了飞速发展,其中所包含的新材料、图案化技术和工艺能以更小的特征尺寸提供更高的器件性能。这些纳米级3D结构对测量领域提出了更大的挑战^[2]。光刻技术在IC制造中的地位至关重要,光刻质量直接影响产品的成品率。而套刻误差作为影响光刻质量的重要因素,其精度要求随着IC制造工艺的发展不断突破,先进节点尺寸也不断减小^[3]。根据经验法则,套刻精度应当优于标称关键尺寸(CD)的20%~30%^[4-5]。

套刻误差是指在掩模版进行曝光时当前层图案和参考层图案之间的位置偏差。目前套刻误差测量方法主要分为基于成像的测量(IFO)方法与基于衍射的测量(DBO)方法两类。其中IFO方法随着节点的不断突破而受到光学显微镜分辨率的限制^[6],且检测时需要不断调整焦距、照射激光波长以提高图像对比度。扫描电子显微镜(SEM)、原子力显微镜(AFM)、扫描隧道显微镜(STM)等传统手段,可以实现高精度测量,但会对器件本身造成损伤^[7-8]。在先进节点工艺中,DBO方法因其受工艺影响更小而获得更广泛的应用,但其发展年限较短,国际上尚未对其展开量值溯源研究,其测量结果可能存在较大误差^[6,9-10]。过焦扫描

光学显微法(TSOM)是一种快速、无损、高可靠性的测量技术。该方法采用光学显微镜获取样品焦平面和不同离焦位置的一组图像,利用该组图像生成样品的三维反射空间光场,再经过处理得到待测信息^[11]。传统基于图像处理的测量方法只采集焦点处的清晰图像用于提取测量结果,其他离焦位置的光场信息被认为是无效信息。该方法的测量分辨率受限于衍射效应影响,在可见光区域的分辨率约为200 nm。事实上,离焦位置的光场信息也可以在一定程度上反映样品结构信息。TSOM利用焦点与离焦位置的三维光场信息,突破光学显微镜分辨率的限制,可在与传统图像测量方法同等硬件条件下提升测量精度^[12-14]。通过将TSOM与机器学习模型相结合,可以避免环境噪声对测量结果的影响,进一步提高测量精度。该方法在高精度微纳测量方面具有广阔的应用场景。

本文提出基于TSOM结合卷积神经网络模型的套刻误差测量方法,采集套刻标识图像,对其生成的TSOM图集进行处理,并在对TSOM图集分析时结合深度学习的方法,对卷积神经网络模型进行训练,实现了对不同样品的套刻误差回归预测。预测结果显示该方法可实现亚纳米级准确度与重复精度,证明了该方法对套刻误差测量的有效性和可行性。该方法具有结构简单、成本低等优点,可为套刻误差测量提供一种新的高精度、无损检测方式。

收稿日期: 2023-12-07; 修回日期: 2024-02-02; 录用日期: 2024-02-26; 网络首发日期: 2024-03-26

基金项目: 国家重点研发计划(2021YFB2012002)、吉林省科技发展计划重点研发项目(20210203156SF)、吉林省教育厅“十三五”科学技术项目(JJKH20190599KJ)、清华大学精密测试技术及仪器国家重点实验室开放基金(TH20-01)

通信作者: *Soldier_1973@163.com; **shijunkai@ime.ac.cn

2 测量原理

2.1 套刻标识偏移量测量

套刻误差描述的是光刻过程中每一层电路图案转移到硅片上的精确程度,所以每一层都要排布套刻标识以确定是否达到工艺要求^[15-16]。图 1(a)为典型的 Bar-in-Bar 套刻标识示意图,其中灰色内框代表前一层,黄色外框代表当前层。标识边长通常为 20~50 μm,线宽一般为 1~3 μm^[17-19]。通过测量内框与外框沿 x 、 y 方向的距离得到 σ_{x_1} 、 σ_{x_2} 、 σ_{y_1} 、 σ_{y_2} ,则沿 x 、 y 方向的套刻误差可表示为

$$\sigma_x = \frac{1}{2}(\sigma_{x_1} - \sigma_{x_2}), \sigma_y = \frac{1}{2}(\sigma_{y_1} - \sigma_{y_2}), \quad (1)$$

最终的套刻误差可表示为

$$\sigma = \sqrt{(\sigma_x^2 + \sigma_y^2)}. \quad (2)$$

如图 1(b)所示,套刻标识一般排布在曝光区域的边缘位置,中间空白部分为曝光加工区域,通过对 4 个位置标识的套刻误差测量值取平均,减小随机误差对测量结果的影响。常用的套刻标识图案均具有旋转对称性,本文仅以套刻标识 x 方向的偏移量测量结果验证所提方法的有效性。

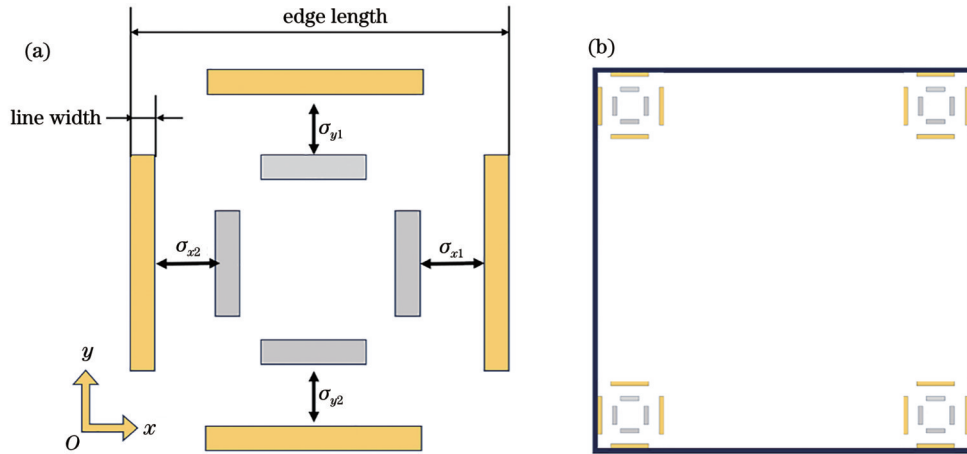


图 1 IBO 标识 Bar-in-Bar。(a) IBO 误差测量方法示意图;(b) IBO 标识位置示意图

Fig. 1 IBO mark Bar-in-Bar. (a) Schematic diagram of measurement method for IBO error; (b) schematic diagram of IBO mark location

2.2 过焦扫描显微测量方法

TSOM 测量过程如图 2 所示。测量装置以光学显微镜(GMM-370,上海光密仪器有限公司)为主体,物镜采用显微镜自带的 60 倍镜头。首先将被测样品放置在显微镜样品台上,由压电陶瓷(PZT, P11.Z300K, 哈尔滨芯明天科技有限公司)驱动样品台沿 z 轴扫描并通过焦点,扫描过程中由

高灵敏度相机(像素 1280 pixel×1024 pixel,像素尺寸 4.65 μm×4.65 μm,DCU224M, Thorlabs)采集一系列不同焦点位置的样品图案,将采集的图像按空间位置堆叠获得 TSOM 三维光场,通过沿 z 轴方向截取三维光场得到包含样品结构信息的 TSOM 图。为了提取待测参数信息,通常采用库匹配法或学习模型方法。

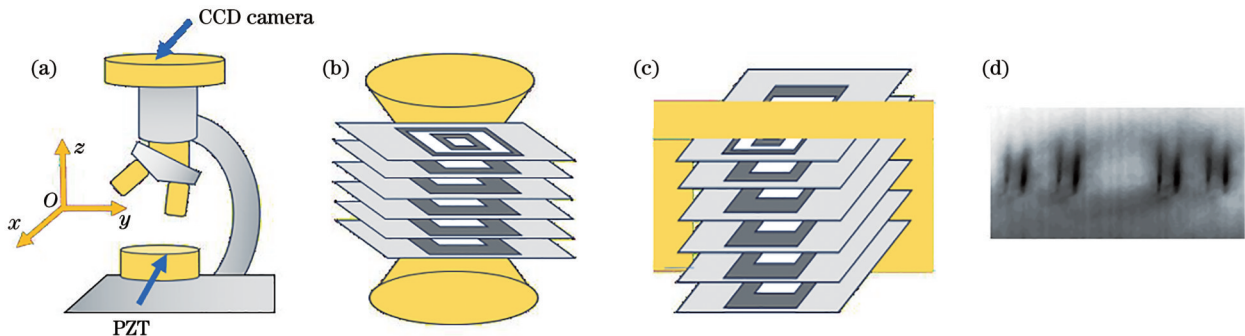


图 2 过焦扫描测量过程示意图。(a)光学显微镜;(b)过焦扫描示意图;(c)截取光学模型垂直剖面;(d)TSOM 图

Fig. 2 Schematic diagram of through-focus scanning measurement process. (a) Optical microscope; (b) schematic diagram of through-focus scanning; (c) captured vertical profile of optical model; (d) TSOM pattern

采用库匹配方法时需要先建立 TSOM 特征库并将其与测量采集生成的 TSOM 图进行匹配,这对仪器

的精度和稳定性要求较高,在分析不确定性因素比较多或未知成分的样品时,该方法的测量效果较差,同时

仿真耗时较长^[20-21]。学习模型法通过学习算法对 TSOM 图进行特征提取,利用 TSOM 数据集训练回归模型,实现对待测参数的预测,学习模型法在 TSOM 测量中将具有更高的精度。

3 深度学习模型

本文基于卷积神经网络(CNN)建立深度学习模型,利用 PyTorch 对 TSOM 图对应的套刻误差进行回

归预测,具体流程如图 3 所示。首先通过实验装置采集图片并生成 TSOM 图,在对 TSOM 图进行处理后建立训练集和测试集,同时构建卷积神经网络模型,并采用均方误差(MSE)损失函数及自适应矩估计(Adam)优化器,通过测试集评估模型预测性能。如果评估结果不符合要求,则需要通过改变激活函数,调整优化器参数、卷积网络层数等超参数重新进行训练,以确定最终的模型参数。

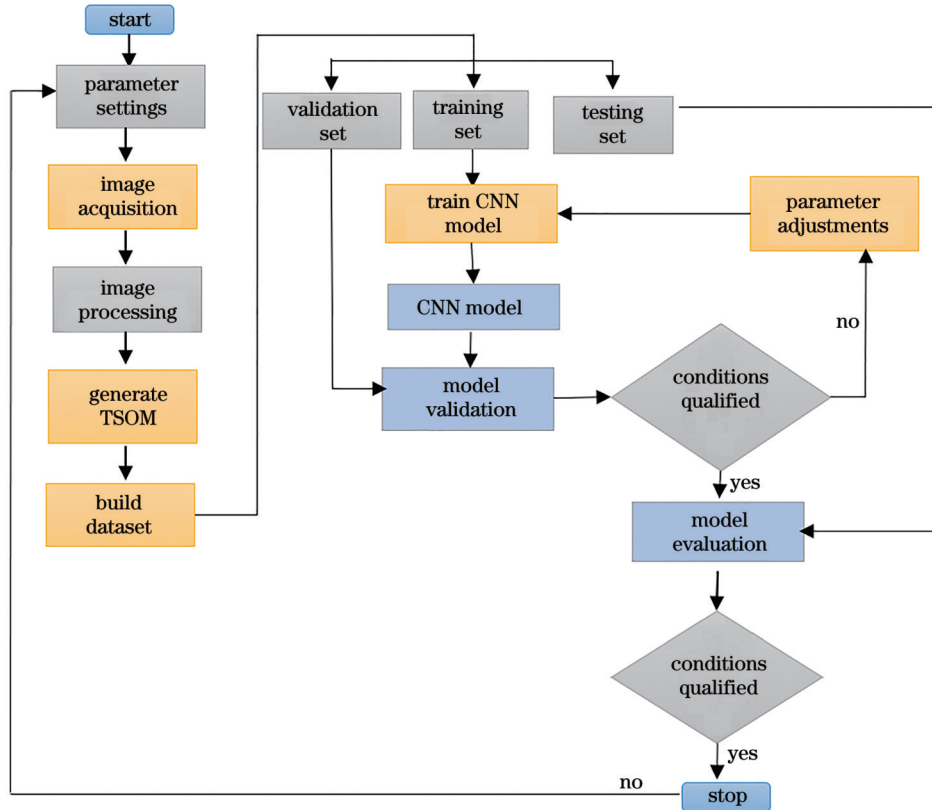


图 3 基于深度学习模型的套刻误差预测流程图

Fig. 3 Overlay error prediction flowchart based on deep learning model

3.1 卷积神经网络

本文使用 Pytorch 搭建 CNN, Pytorch 是属于 Python 平台的深度学习框架,提供了构建、训练深度学习模型的工具和接口,具有高效性、易用性,卷积神

经网络被广泛用于图像、语音识别等场合^[22-23]。CNN 结构通常包含输入层、卷积层、池化层、激活层、全连接层以及输出层。本文采用的网络结构如图 4 所示, TSOM 图以单通道灰度图输入到网络结构中,经过 4

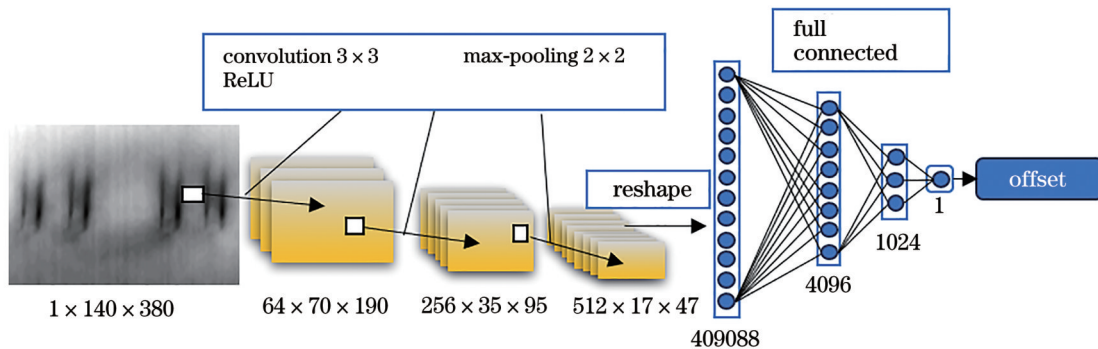


图 4 神经网络结构

Fig. 4 Neural network structure

层卷积层、3层池化层、3层激活层和3层全连接层得到最终结果,具体参数如表1所示。

表1 网络参数
Table 1 Network parameters

Layer	(Input channel number, output channel number)	Kernel size	Stride	Input	Output
Convolution	(1, 64)	(3, 3)	(1, 1)	(1, 140, 380)	(64, 140, 38)
ReLU (Maxpool)	(64, 64)	(2, 2)	(2, 2)	(64, 140, 380)	(64, 70, 190)
Convolution	(64, 256)	(3, 3)	(1, 1)	(64, 70, 190)	(256, 70, 190)
ReLU (Maxpool)	(256, 256)	(2, 2)	(2, 2)	(256, 70, 190)	(256, 35, 95)
Convolution	(256, 512)	(3, 3)	(1, 1)	(256, 35, 95)	(512, 35, 95)
ReLU (Maxpool)	(512, 512)	(2, 2)	(2, 2)	(512, 35, 95)	(512, 17, 47)
Linear	—	—	—	512×17×47	4096
Linear	—	—	—	4096	1024
Linear	—	—	—	1024	1

将 TSOM 图输入到卷积层中进行卷积操作,其公式如下:

$$H_{out} = \frac{H_{in} + 2 \times P_H - D_H \times (K_H - 1)}{S_H} + 1, \quad (3)$$

$$W_{out} = \frac{W_{in} + 2 \times P_W - D_W \times (K_W - 1)}{S_W} + 1, \quad (4)$$

式中: H_{in} 、 H_{out} 分别为图片输入、输出的高度; W_{in} 、 W_{out} 分别为图片输入、输出的宽度; P_H 、 P_W 表示卷积时高度、宽度的填充值; D_H 、 D_W 为控制窗口中元素步幅的参数,默认为1; K_H 、 K_W 为卷积核; S_H 、 S_W 为卷积步长。

ReLU 函数在输入 M 大于 0 时直接输出该值,在输入 M 小于等于 0 时输出 0,公式如下:

$$f(x) = \max(0, M). \quad (5)$$

CNN 学习的目的是通过调整权重参数,使模型输出接近原始特征输入。损失函数是在神经网络学习中反映网络性能损失大小的指标,表示神经网络对监督数据的拟合程度,训练的过程即寻找损失函数最小值

的过程^[24]。当找到最小值时,模型将参数向前传播,重新训练神经网络,使损失达到最小。本文中采用均方误差(MSE)作为损失函数来寻找最小值,其表达式为

$$f_{loss}(\hat{y}, y) = \frac{1}{n} \sum_{i=0}^n (\hat{y}_i - y_i)^2, \quad (6)$$

式中: \hat{y} 和 y 分别为预测值和真值; n 为训练一次所选取的数据样本个数; i 为样品序号; y_i 代表第 i 个实验样品的真值; \hat{y}_i 代表第 i 个实验样品的实际预测值。选择 Adam 优化器来更新参数,最终确定训练模型的 epoch 设置为 500,学习率为 0.001,使拟合效果达到最佳。

3.2 数据集建立

通过显微镜采集套刻标识样品图片,生成 TSOM 图集用于训练模型、优化模型参数和评估模型性能。实验样品共分 4 组,边长和线宽分别为 26 μm 和 2 μm 。样品 x 方向偏移量由光学套刻测量系统 Archer 100 测得(表 2),4 组样品的偏移量间隔分别约为 200、100、50、20 nm。

表2 样品参数
Table 2 Sample parameters

No.	Side length / μm	Linewidth / μm	Offset / nm	Offset interval / nm
1	26	2	-598.51, -399.69, -199.68, -0.13, 199.59, 399.67, 599.37	200
2	26	2	-299.01, -199.21, -100.30, -0.05, 99.60, 200.04, 299.89	100
3	26	2	-149.60, -100.02, -49.15, 0.41, 49.32, 100.46, 151.01	50
4	26	2	-57.70, -39.43, -18.71, 0.23, 20.98, 40.50, 61.06	20

数据集获取流程如图 5 所示,样品沿 z 轴扫描,扫描步长设置为 0.5 μm ,移动范围设置为 70 μm ,流程包含样品从失焦到聚焦再到失焦的过程,每次移动后 CCD 相机采集一幅图像,得到套刻标识初始图像。在靠近套刻标识中心位置处选择图像不同行像素(图 5

中直线)构成 TSOM 图。将得到的 TSOM 图进行分类并建立标签,将其作为最终深度学习模型的训练集、验证集、测试集。对每组各个偏移量样品分别重复测量 15 次,用于生成该组样品的训练集与验证集。其中:训练集含 2016 幅 TSOM 图,用于训练模型;验证

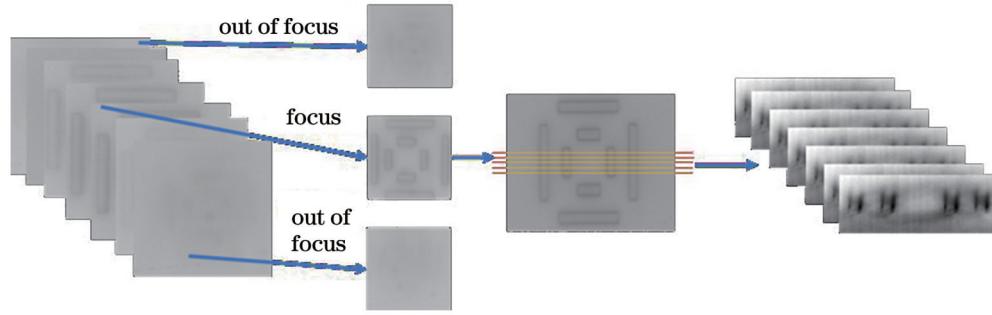


图 5 数据集获取流程

Fig. 5 Dataset acquisition process

集含 210 幅 TSOM 图,用于优化模型参数。对该组样品重复测量 10 次,生成测试集的 280 幅 TSOM 图,用于评估模型预测结果的准确性。

4 实验结果与分析

按照上述流程建立 TSOM 数据集,训练卷积神经网络模型并优化模型参数。利用模型对测试集中

TSOM 图对应的偏移量进行预测,预测结果如图 6 所示。图 6(a)~(d)分别为采用偏移量间隔为 200、100、50、20 nm 的样品进行训练后模型的预测结果,图中实线为模型预测的偏移量值,虚线为偏移量真值。从 4 组结果可以看出,对于不同偏移量样品训练的模型,预测结果曲线与真值曲线接近重合,这表明该训练模型能够准确地预测套刻误差。

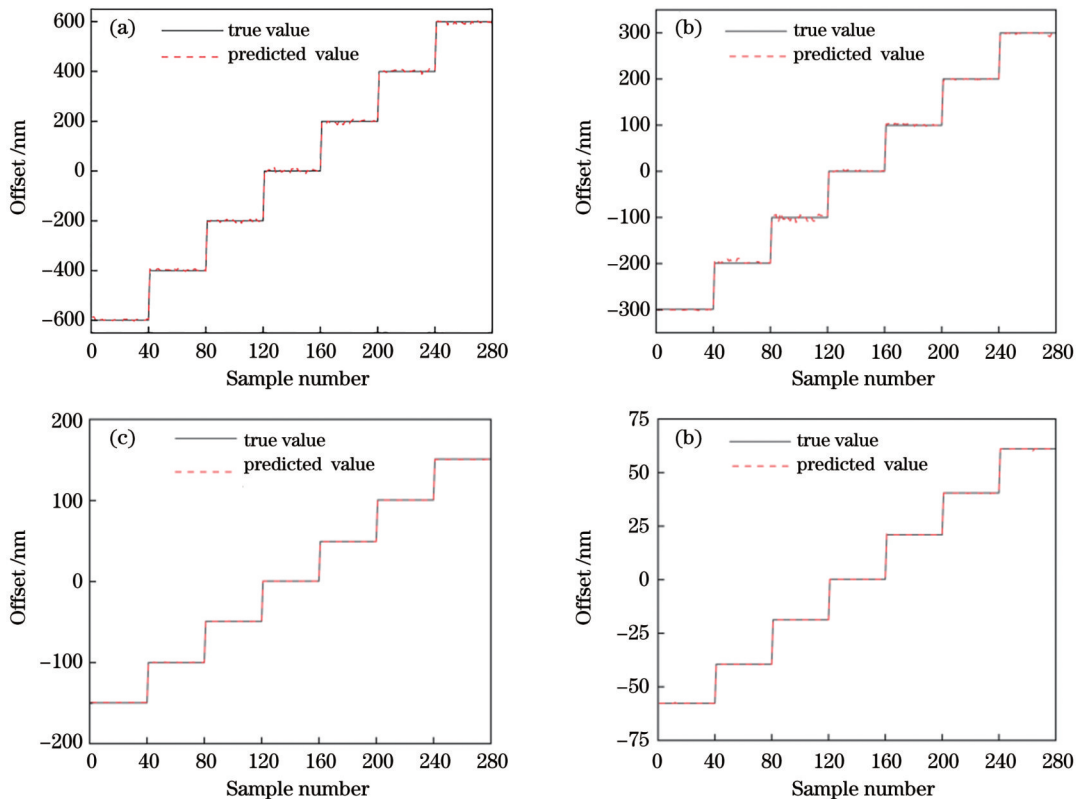


图 6 不同偏移量间隔模型预测结果。(a)间隔 200 nm;(b)间隔 100 nm;(c)间隔 50 nm;(d)间隔 20 nm

Fig. 6 Model prediction results for different step size of offset. (a) Step size is 200 nm; (b) step size is 100 nm; (c) step size is 50 nm; (d) step size is 20 nm

为了进一步评估模型预测值与真值的偏差大小,引入平均绝对误差(MAE)、均方根误差(RMSE)、决定系数 R^2 作为衡量模型预测性能的指标,其中 MAE、RMSE 是通过计算真值和预测值之间的差异来评估模型精度, R^2 是对线性回归模型的一种衡量指

标: R^2 值越接近于 1,说明模型拟合效果越好; R^2 值越接近于 0,则模型拟合效果越差。三个参数的计算公式分别为

$$f_{MAE} = \frac{1}{n} \sum_{i=1}^n |y_i - \hat{y}_i|, \quad (7)$$

$$f_{\text{RMSE}} = \sqrt{\frac{1}{n} \sum_{i=1}^n (y_i - \hat{y}_i)^2}, \quad (8)$$

$$R^2 = 1 - \frac{\sum_{i=1}^n (y_i - \hat{y}_i)^2}{\sum_{i=1}^n (y_i - \bar{y})^2}, \quad (9)$$

式中： \bar{y} 代表 n 个实验样品的预测结果的平均值。图 7 为 4 组样品偏移量预测值的评价结果，左侧纵坐标是 MAE 和 RMSE 值，右侧纵坐标是 R^2 值，横坐标是样品偏移量间隔，可以看到，4 组样品的 R^2 值均大于 0.9995，表明模型具有极高的拟合精度。当样品偏移量间隔为 200 nm 时，MAE 值和 RMSE 值分别为 4.2 nm 和 5.3 nm。随着偏移量间隔的减小，MAE 值和 RMSE 值均呈线性下降。当偏移量间隔为 20 nm 时，偏移量

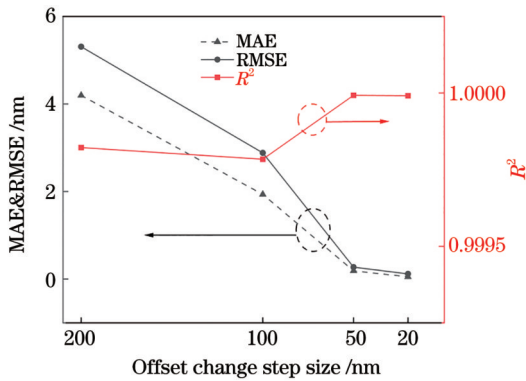
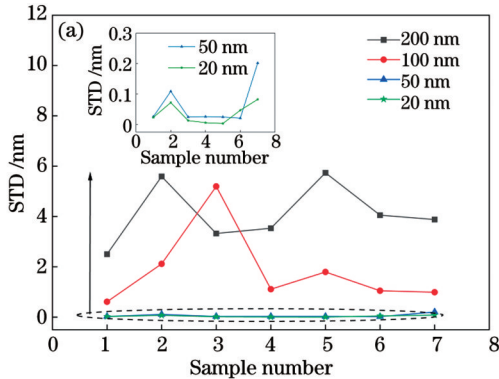


图 7 模型预测性能评价指标

Fig. 7 Evaluation indicators of model prediction performance



预测结果的 MAE 值和 RMSE 值减小到 0.05 nm 和 0.12 nm。这是因为训练样品偏移量间隔减小，深度学习标签值间隔随之减小，测量分辨率得到提升。

采用 3 倍标准差 (STD) 来评价测量系统的重复精度，标准差的计算公式为

$$S(x) = \sqrt{\frac{\sum_{j=1}^k (x_j - \bar{x})^2}{k-1}}, \quad (10)$$

式中： $S(x)$ 为标准差； x_j 为第 j 次测量的结果； k 为测量次数； \bar{x} 为 k 次测量结果的平均值。对实验样品重复测量 10 次，使用模型预测结果，通过计算 STD 来验证重复性，结果如图 8(a) 所示。4 组样品的 STD 值均在 6 nm 以下，对应的测量重复精度 (3σ) 为 18 nm。随着样品偏移量间隔的减小，测量重复精度也呈现明显的下降趋势，这说明训练样品偏移量间隔同样也会影响预测结果的重复性。当偏移量间隔减小到 20 nm 时，套刻误差测量结果的 STD 值均优于 0.083 nm [图 8(a) 中插图]，对应的测量重复精度 (3σ) 为 0.25 nm，该指标与光学套刻测量系统 Archer 100 的重复性测量结果相当。该组样品相应的实测值与误差值如图 8(b) 所示，可以看出该组样品的测量误差均优于 0.1 nm，模型预测结果表现出极高的准确性与很好的重复性。实验结果表明，TSOM 结合深度学习模型的方法可以准确地预测套刻标识的偏移量。根据实验结果，采用偏移量间隔更小的样品训练模型，可以进一步提高套刻误差测量结果的准确度和重复精度。

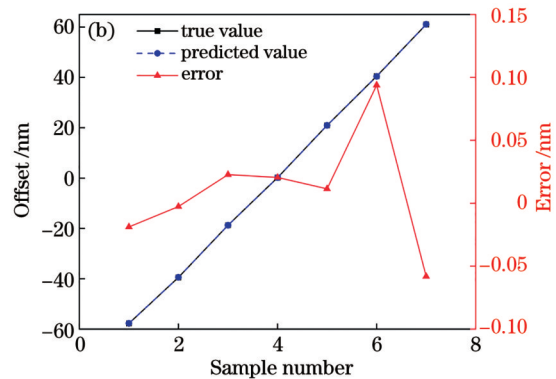


图 8 模型单点重复性测量结果。(a) 总体样品 STD 值；(b) 0.02 μm 样品测量结果

Fig. 8 Measurement results of single-point repeatability of model. (a) Overall sample STD values; (b) measurement results of 0.02 μm sample

5 结 论

本文基于过焦扫描显微测量方法，结合深度学习模型实现了对 Bar-in-Bar 套刻标识偏移量的测量。区别于传统 IBO 方法，本文利用光学显微镜采集一组不同焦点的图像，生成 TSOM 图集，建立卷积网络模型以进行训练验证，节省测量仿真时间，实现对套刻标识偏移量的回归预测。采用偏移量间隔为 20 nm 的套刻

标识样品用于模型训练，得到的测量误差小于 0.1 nm，重复精度 (3σ) 优于 0.25 nm。实验结果表明该方法可以实现亚纳米级套刻误差测量。该方法适用于多种类型的套刻标识，可为套刻误差测量提供一种新的测量手段。

参 考 文 献

- [1] 曲永义, 李先军. 创新链赶超: 中国集成电路产业的创新与发

- 展[J]. 经济管理, 2022, 44(9): 5-26.
- Qu Y Y, Li X J. Innovation chain catches up: innovation and development of China's IC industry[J]. Business Management Journal, 2022, 44(9): 5-26.
- [2] International Roadmap for Devices and Systems (IRDS™) [EB/OL]. [2021-05-04]. <https://irds.ieee.org/editions/2018/yield-enhancement>.
- [3] Lin N, Chen Y Y, Wei X, et al. Spectral purity systems applied for laser-produced plasma extreme ultraviolet lithography sources: a review[J]. High Power Laser Science and Engineering, 2023, 11: e64.
- [4] den Boef A J. Optical wafer metrology sensors for process-robust CD and overlay control in semiconductor device manufacturing[J]. Surface Topography: Metrology and Properties, 2016, 4(2): 023001.
- [5] 邱俊, 杨光华, 李璟, 等. 光刻对准关键技术的发展与挑战[J]. 光学学报, 2023, 43(19): 1900001.
- Qiu J, Yang G H, Li J, et al. Development and challenges of lithographical alignment technologies[J]. Acta Optica Sinica, 2023, 43(19): 1900001.
- [6] 李一鸣, 杨霖, 王晓浩, 等. 光刻套刻误差测量技术[J]. 激光与光电子学进展, 2022, 59(9): 0922023.
- Li Y M, Yang L, Wang X H, et al. Overlay metrology for lithography machine[J]. Laser & Optoelectronics Progress, 2022, 59(9): 0922023.
- [7] Liu H C, Osborne J R, Dahlen G A, et al. Recent CD AFM probe developments for sub-45 nm technology nodes[J]. Proceedings of SPIE, 2008, 6922: 69222J.
- [8] 王娜, 刘立拓, 宋晓娇, 等. 基于过焦扫描光学显微镜的光学元件亚表面缺陷检测方法[J]. 光学学报, 2023, 43(21): 2112001.
- Wang N, Liu L T, Song X J, et al. Subsurface defect detection method of optical elements based on through-focus scanning optical microscopy[J]. Acta Optica Sinica, 2023, 43(21): 2112001.
- [9] Saravanan C S, Liu Y D, Dasari P, et al. Evaluating diffraction based overlay metrology for double patterning technologies[J]. Proceedings of SPIE, 2008, 6922: 69220C.
- [10] Saravanan C S, Tan A, Dasari P, et al. Diffraction based overlay metrology for α -carbon applications[J]. Proceedings of SPIE, 2008, 6922: 69222W.
- [11] Attota R, Germer T A, Silver R M. Through-focus scanning-optical-microscope imaging method for nanoscale dimensional analysis[J]. Optics Letters, 2008, 33(17): 1990-1992.
- [12] Attota R, Silver R, Barnes B M. Optical through-focus technique that differentiates small changes in line width, line height, and sidewall angle for CD, overlay, and defect metrology applications[J]. Proceedings of SPIE, 2008, 6922: 69220F.
- [13] Attota R, Seiler D G, Diebold A C, et al. TSOM method for nanoelectronics dimensional metrology[C]. AIP Conference Proceedings, 2011, 1395: 57-63.
- [14] Attota R, Dixson R G, Vladár A E. Through-focus scanning optical microscopy[J]. Proceedings of SPIE, 2011, 8036: 803610.
- [15] 杜聚有, 戴凤钊, 步扬, 等. 基于自相干叠栅条纹的光刻机对准技术[J]. 中国激光, 2017, 44(12): 1204006.
- Du J Y, Dai F Z, Bu Y, et al. Alignment technique using moire fringes based on self-coherence in lithographic tools[J]. Chinese Journal of Lasers, 2017, 44(12): 1204006.
- [16] Troccoli P M, Smith N P, Zantow T. Tool and mark design factors that influence optical overlay measurement errors[J]. Proceedings of SPIE, 1992, 1673: 148-156.
- [17] Nam Y S, Kim S, Shin J H, et al. Overlay improvement methods with diffraction based overlay and integrated metrology [J]. Proceedings of SPIE, 2015, 9426: 942612.
- [18] Rigolli P L, Rozzoni L, Turco C, et al. AIM technology for non-volatile memories microelectronics devices[J]. Proceedings of SPIE, 2006, 6152: 61524C.
- [19] Ausschnitt C P, Chu W, Kolor D, et al. Blossom overlay metrology implementation[J]. Proceedings of SPIE, 2007, 6518: 65180G.
- [20] Attota R K. Through-focus or volumetric type of optical imaging methods: a review[J]. Journal of Biomedical Optics, 2018, 23(7): 070901.
- [21] Lee J H, Park J H, Jeong D, et al. Tip/tilt-compensated through-focus scanning optical microscopy[J]. Proceedings of SPIE, 2016, 10023: 100230P.
- [22] Girshick R, Donahue J, Darrell T, et al. Rich feature hierarchies for accurate object detection and semantic segmentation[C]//Proceedings of the 2014 IEEE Conference on Computer Vision and Pattern Recognition, June 23–28, 2014, Columbus, OH, USA. New York: IEEE Press, 2014: 580-587.
- [23] Wang F, Wang H, Wang H C, et al. Learning from simulation: an end-to-end deep-learning approach for computational ghost imaging[J]. Optics Express, 2019, 27(18): 25560-25572.
- [24] Ning X, Tian W J, Yu Z Y, et al. HCFNN: high-order coverage function neural network for image classification[J]. Pattern Recognition, 2022, 131: 108873.

Overlay Error Measurement Method Based on Through-Focus Scanning Optical Microscopy

Liu Hao¹, Wang Jinsong^{1*}, Shi Junkai^{2***}, Li Guannan², Chen Xiaomei², Zhou Weihu²

¹School of Optoelectronic Engineering, Changchun University of Science and Technology, Changchun 130022, Jilin, China;

²Optoelectronic Technology R&D Center, Institute of Microelectronics of the Chinese Academy of Sciences,

Beijing 100029, China

Abstract

Objective Over the past decade, integrated circuit (IC) technology has experienced remarkable advancements through the use of complex three-dimensional (3D) device structures, including new materials, patterning techniques, and processes

that provide higher device performance with reduced feature sizes. These nanoscale 3D structures present significant challenges to the field of measurement. Lithography technology plays an important role in IC manufacturing, and its quality directly affects the yield of products. As an important factor affecting the quality of lithography, the precision requirements of overlay error have become increasingly stringent with the continuous breakthrough of the IC manufacturing process and the continuous reduction of advanced node sizes. According to the rule of thumb, the overlay accuracy should be better than 20%–30% of the critical dimension (CD). Currently, the measurement methods of overlay error are mainly divided into two categories: image-based overlay (IBO) and diffraction-based overlay (DBO). The IBO method is limited by the resolution of the optical microscope with the continuous breakthrough of the node, and the focal length and the laser wavelength need to be adjusted to enhance image contrast. There is no research on the traceability of the DBO method, which may result in large measurement errors. Through-focus scanning optical microscope (TSOM) is a fast, non-destructive, and highly reliable measurement technique. In order to realize the rapid non-destructive detection of the overlay error, a novel method for detecting the overlay error using the TSOM was proposed and explored in detail. This innovative approach aims to enhance the accuracy and efficiency of overlay error measurements, ultimately contributing to the advancement of IC technology.

Methods The sample was placed on a microscope sample stage, which was driven by a piezoelectric transducer (PZT) to facilitate scanning along the Z -axis and through the focus point. During the scanning process, a series of sample patterns at different focus positions were captured by a charge-coupled device (CCD) camera. These images were then stacked based on their spatial positions to obtain a TSOM 3D light field. By intercepting the 3D light field along the Z -axis direction, a TSOM map containing the structural information of the sample was generated. After the TSOM map was processed, the train set and test set were established, and a convolutional neural network (CNN) model was constructed. The mean square error (MSE) loss function and adaptive moment estimation (Adam) optimizer were used to evaluate the prediction performance of the model through the test set. If the evaluation results did not meet the desired criteria, it was necessary to retrain the hyperparameters, such as the optimizer parameters and the number of convolutional network layers, by changing the activation function to determine the final model parameters. The information of the parameters to be tested was extracted by deep learning model prediction.

Results and Discussions This method enables accurate prediction of overlay errors. For the model trained by different offset samples, the predicted result curve closely resembles the true value curve (Fig. 6). When the sample offset interval is 200 nm, the mean absolute error (MAE) and root mean square error (RMSE) values are 4.2 nm and 5.3 nm, respectively. As the offset interval decreases, both the MAE and RMSE values decrease linearly (Fig. 7). When the offset interval is reduced to 20 nm, the MAE and RMSE values of the offset prediction results are further reduced to 0.05 nm and 0.12 nm, respectively. This can be explained by the fact that as the offset interval of training samples decreases, the interval of deep learning label value decreases, and measurement resolution is enhanced. The standard deviation (STD) values of the four groups of samples are all below 6 nm and show a significant downward trend with the decrease in the offset interval of samples, which indicates that the offset interval of samples will also affect the repeatability of the prediction results. When the offset interval is reduced to 20 nm, the STD values of the overlay error measurement results are better than 0.083 nm (Fig. 8), and the corresponding repeatability accuracy (3σ) is 0.25 nm. By using a smaller interval of experimental samples, higher measurement accuracy can be achieved.

Conclusions The measurement of Bar-in-Bar marking offset is realized based on TSOM combined with a deep learning model. Unlike the traditional IBO method, we utilize an optical microscope to capture a series of images at different focal points, generating a TSOM atlas. A convolutional neural network model is then established for training and verification, which saves measurement simulation time and enables the regression prediction of the overlay marking offset. The sample with an offset interval of 20 nm is used for model training. The measurement accuracy is superior to 0.1 nm, and the repeatability accuracy (3σ) is superior to 0.25 nm. The experimental results show that this method is capable of measuring sub-nanometer overlay errors and is suitable for various types of overlay markings. In addition, it has a simple structure and low cost, which serves as a novel measurement method for overlay error measurement.

Key words measurement; overlay error; through-focus scanning optical microscopy; deep learning; non-destructive testing